JOURNAL OF VIROLOGY, Nov. 1997, p. 8572–8581 Vol. 71, No. 11
0022-538X/97/$04.00+0

Alterations in Catalytic Activity and Virus Maturation Produced by Mutation of the Conserved Histidine Residues of Herpes Simplex Virus Type 1 Protease

R. BRUCE REGISTER AND JULES A. SHAFER*

Department of Biological Chemistry, Merck Research Laboratories, West Point, Pennsylvania 19486

Received 29 July 1997/Accepted 1 August 1997

Mutant herpes simplex virus type 1 (HSV-1) viruses were constructed to characterize the roles of the conserved histidine residues (H61 and H148) of HSV-1 protease in the regulation of catalytic activity and virus maturation. Viruses containing mutations at H61 (H61V-V711, H61Y-V715, and H61A-V730) were unable to grow on Vero cells. These mutant viruses could process neither Pra to N_0 nor ICP-35cd to ICP-35ef. Transmission electron microscopy studies of H61A-V730-infected Vero cells indicated that capsid maturation is arrested at a state characterized by the predominance of large symmetrical arrays of B capsids within the nucleus. Two mutations at H148 (in viruses H148A-V712 and H148E-V728) gave rise to mutant viruses that grew with a small-plaque phenotype; one of the viruses, H148E-V728, was particularly attenuated when grown at a low multiplicity of infection. The rate of processing of Pra to N_0 in infected Vero cells increased in the order H148A-V712 < H148E-V728 < parental strain HSV-1-V731. The observation that H148A-V712 processes Pra to N_0 and ICP-35cd to ICP-35ef, whereas H61A does not, establishes H61 as the catalytically essential conserved His assuming that HSV-1 protease, like other serine proteases, utilizes an active-site histidine residue in catalysis. Two of the mutations at H148 (viruses H148K-V729 and H148Y-V716) produced nonviable viruses. H148K-V729 processed neither Pra to N_0 nor ICP-35cd to ICP-35ef, whereas H148Y-V716 processed Pra to N_0 but did not process ICP-35cd to ICP-35ef. The range of phenotypes observed with the H148 mutant viruses suggests that residue 148 of the HSV-1 protease is a determinant of virus growth rate and viability because of its effects on the activity of the protease and/or the role of the protease domain in capsid assembly and DNA packaging.

Herpes simplex virus type 1 (HSV-1) is a large double-stranded DNA virus that replicates in the nucleus of a host cell. The virus has a system of capsid assembly that appears similar to that of bacterial phage, wherein the capsid is assembled around a protein scaffold (11). Two proteins encoded by the overlapping genes UL26 and UL26.5 (Fig. 1) constitute the scaffold of the HSV-1 capsid. UL26 encodes the 635-amino-acid protease (Pra). UL26.5 encodes the assembly protein, infected-cell protein 35 (ICP-35cd), with its coding region starting in frame with that of the Pra gene at the codon for residue M307 and coterminating with that of the Pra gene (13, 14).

The viral capsid, consisting of VP5, VP19C, VP23, and VP26 and a core with a 1:10 ratio of Pra to ICP-35cd assembles in the nucleus (17, 18). The presence of either Pra or ICP-35cd is sufficient to ensure capsid formation (6, 7, 16, 25, 26). Virus lacking an active protease, however, is blocked from entering the next phase of virus maturation: digestion and packaging of HSV-1 genomic DNA (8). Upon capsid assembly the protease becomes active and cleaves itself twice at amino acid residues A247, the release site, and A610, the maturation site (Fig. 1). ICP-35cd is also cleaved by the protease at the homologous maturation site to generate ICP-35ef. The protease-catalyzed cleavages result in depolymerization of the protease-assembly protein complex releasing processed ICP-35ef and N_b (the C terminus of Pra) from the capsid interior. N_0, the proteolytically active domain of Pra (amino acid residues 1 to 247), is retained within the capsid. HSV-1 genomic DNA is packaged either concurrently with or subsequent to HSV-1 protease-catalyzed cleavage of ICP-35cd to ICP-35ef.

HSV-1 protease is a serine protease as defined by its reaction with the inhibitors DFP (diisopropylfluorophosphate), phenylmethylsulfonyl fluoride, and chymostatin (12). Dilanni et al. (7) identified S129 as the active-site serine based upon the manner of its labeling with [^{3}H]DFP. The active-site histidine of the serine protease commonly present in other serine proteases has not been definitively defined. Sequence alignments of α, β, and γ herpes virus protease homologs revealed two conserved histidine residues, either of which may be the catalytically essential His (29) assuming that the herpes protease, like other serine proteases, utilizes an active-site histidine residue as a general acid or base for catalysis. These residues are H61 and H148 in HSV-1 protease and H47 and H142 in simian cytomegalovirus (sCMV) protease. The observation that sCMV protease mutants H142A and H142E exhibit low but detectable levels of protease activity, whereas the H47A mutant protease is completely devoid of activity (29), suggests that H47 is the catalytically essential His residue of sCMV protease and that, by analogy, H61 is the catalytically essential His of HSV-1 protease. Recent X-ray diffraction analyses of human CMV (hCMV) protease crystals (2, 21, 24, 27) indicate that H63 (homologous to H47 and H61 of sCMV and HSV-1, respectively) in hCMV is indeed H-bonded to the active-site Ser residue as expected for an active-site histidine residue. Surprisingly, the other conserved histidine residue, H157 of hCMV, appears to be H-bonded to H63 as if it were replacing the aspartic acid residue in the catalytic triad of conventional serine proteases. In contrast to what was found from observations of sCMV protease, point mutations in HSV-1 protease at either HSV-1 H61 or H148 have been

* Corresponding author. Mailing address: Department of Biological Chemistry, Merck Research Laboratories, West Point, PA 19486. Phone: (215) 652-7203. Fax: (215) 652-3082.

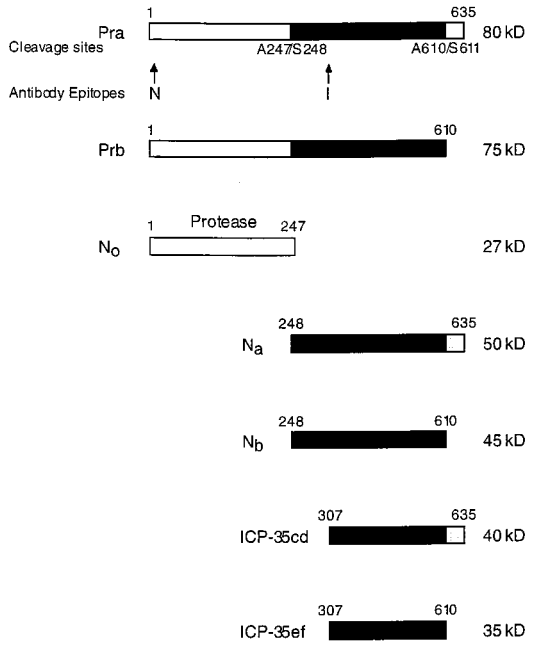

FIG. 1. HSV-1 protease cleavage sites. HSV-1 protease (Pra) is a 635-amino-acid serine protease that undergoes autocatalytic cleavage at Ala247 and Ala610. The products of these cleavages are N_0 (amino acids [aa] 1 to 247), which contains the protease activity, N_a (aa 248 to 635), and N_b (aa 248 to 610). The assembly protein, ICP-35cd, starts in frame with the protease at M307 and is coterminal with it at residue 635. The protease also acts upon ICP-35cd at residue 610 to yield ICP-35ef. The locations of the epitopes recognized by the antibodies used in this study are designated by the letters N and I. kD, kilodaltons.

reported to result in the loss of HSV-1 protease activity in vitro (12). Thus, assignment of the catalytically essential His of HSV-1 protease has not been possible.

In the present study we used our two-plasmid, four-cosmid system of mutagenesis (22) to construct HSV-1 mutants and to determine, for the first time in the context of the virus, the effects of mutations at H61 and H148 in the protease Pra.

(Part of this work was taken from a Ph.D. thesis submitted by R. B. Register to the graduate school of Hahnemann University.)

MATERIALS AND METHODS

PCR mutagenesis. Each mutated negative-strand oligonucleotide A listed below was paired with a positive-strand oligonucleotide homologous to DNA 5′ of the first *Bsm*I site (5′-GTACTCAAAAGGTCATAC-3′), and each positive-strand mutated oligonucleotide B listed below was paired with a negative-strand oligonucleotide homologous to DNA 3′ of the second *Bsm*I site (5′-GGGAAA CCAAACGCGGAATG-3′). PCR mutagenesis was then carried out on plasmid pRHS2 as previously described (10, 22). The mutated PCR *Bsm*I fragments of the protease gene were subcloned into plasmid vector pR700 and employed in the construction of mutant virus by using the two-plasmid, four-cosmid system of mutagenesis previously described by us (22). The viruses and associated oligonucleotides are as follows. H61V-V711 (new *Aat*II site): A, 5′-CCTCGCAGC CAGCGCGGACGTCCACGTTAATCGGGAGTGGG-3′; B, 5′-CCCACTCC CGATTAACGTGGACGTCCGCGCTGGCTGCGAGGTG-3′; H61Y-V715; A, 5′-CGCGGTAGTCCACGTTA-3′; B, 5′-CCCACTCCCGATTAACGTGGA CTACCGCGCTGGCTGCGAGGTG-3′; H61A-V730 (new *Psp*1406I site): A, 5′-CAGCCAGCGCGGGCGTCAACGTTAATCGGGAGTGGG-3′; B, 5′-CC GATTAACGTTGACGCCCGCGCTGGCTGCGAGGTGGG-3′; H148A-V712 (new *Pst*I site): A, 5′-GATCGCGCACAGCGCGACTGCAGCGAACAGCGT GCGATCGGGG-3′; B, 5′-CCCGATCGCACGCTGTTCGCTGCAGTCGCG CTGTGCGCGATCGGGCGG-3′; H148Y-V716; A, 5′-GCGACGTACGCGA ACAGC-3′; B, 5′-CCCCGATCGCACGCTGTTCGCGTACGTCGCGCTGT GCGCGATCGG-3′; H148E-V728 (new *Eco*47III site): A, 5′-CGCACAGCGC TACTTCCGCGAACAGCGTGCGATCGGG-3′; B, 5′-CTGTTCGCGGAAG TAGCGCTGTGCGCGATCGG-3′; H148K-V729 (new *Sty*I site): A, 5′-CACA GCGCGACCTTGGCGAACAGCGTGCGATCGGG-3′; B, 5′-CGCTGTTCG CCAAGGTCGCGCTGTGCGCGATCG-3′.

Cosmid vectors. cos6, cos14, cos28, cos48, and cos56 obtained from Cunningham and Davison were previously described (3).

Plasmids. pRHS2 consisting of HSV-1 strain F DNA, base pairs 49126 to 53273, starting within UL25 and ending within UL27; pR700 consisting of HSV-1 strain 17 DNA, base pairs 44440 to 57747, starting within UL22 and ending within UL28; and pR710 consisting of HSV-1 strain 17 DNA, base pairs 24699 to 49435, starting between UL10 and UL11 and ending within UL25, have been previously described (22).

Characterization of mutations. All of the PCR *Bsm*I mutant fragments (1,127 base pairs) were sequenced to confirm that no second-site mutations were introduced during the mutagenesis procedure. In addition, to confirm the presence of the mutations in the virus a new restriction endonuclease site was added at the site of mutation (with the exception of mutants H61Y-V715 and H148Y-V716). The DNA of each of the mutant viruses was digested with the restriction endonuclease corresponding to the amino acid mutation and compared with the wild-type HSV-1 genomic DNA by Southern analysis (data not shown). DNA from mutants H61Y-V715 and H148Y-V716 was digested with *Bsm*I and was shown to contain this fragment. It might be argued that the recombinant mutant virus suffered a second-site mutation that conferred the phenotype(s) described in this paper. To assess this possibility, at least three separate transfections were performed for each mutation and the phenotypes of the resulting viruses were compared. Additionally, two of the *Bsm*I fragments containing mutated protease gene N_0, i.e., those from H61A-V730 and H148A-V712, were subcloned from the mutant viruses and sequenced.

Host range cell line PHS-23. This cell line, which expresses the HSV-1 strain F Pra upon HSV infection, has been previously described (22).

Parental HSV-1-V731 virus strain. The parental virus (HSV-1-V731) used in this study is a strain 17 virus wherein a strain F *Bsm*I fragment encoding N_0 replaces the corresponding *Bsm*I fragment of strain 17. Use of this chimeric parental strain was prompted by the ready availability of the strain 17 cosmids, together with the fact that previous studies of the effect of protease mutations in N_0 were performed with strain F protease. HSV-1 strain 17 and chimeric parental strain HSV-1-V731 were compared with respect to growth curves at 31, 34, 37, and 39°C. Moreover, protease activity was assessed by Western blot analysis. No differences between HSV-1 strain 17 and HSV-1-V731 with respect to growth characteristics or protease activity were observed (data not shown).

Transfections. Previously described (22) transfection procedures were used to create mutant virus. Mutant viruses derived from PCR-mutated Pra-encoding plasmids are designated by the numbers of the plasmid constructs encoding Pra that were used to construct the mutant viruses, with the letter "V" substituted for "pR."

Growth and plaque assays. One-step growth curves of mutant viruses H148A-V712 and H148E-V728 were performed at both a low multiplicity of infection (MOI) (0.0005 PFU/cell) and a high MOI (3 PFU/cell). Six-well clusters were set up with 1.0×10^5 Vero cells the day before infection in triplicate for each time point. Each well was infected with either 150 to 200 PFU (low-MOI) or 3.0×10^5 PFU (high-MOI) of virus in 1 ml. In the low-MOI experiment one set of clusters was washed 1 h postinfection and refed with 1× Dulbecco modified Eagle medium, 2% fetal calf serum, and 1% human immunoglobulin G (Armour). Two to four days postinfection these clusters were fixed with methanol and stained with Accustain (Sigma) and total plaques were counted. In the high-MOI experiment, the 1.5×10^6-PFU/ml virus stock was serially diluted to confirm the titer. The second set of clusters in each experiment was frozen at 4, 8, 10 (high-MOI experiment only), 12, 16, and 20 h postinfection. The clusters were then thawed and sonicated, and the titers for each well (three wells per time point) were determined in duplicate.

Antibodies. The antibodies (a gift from A. Conley of Merck Research Laboratories) were raised in rabbits, with a keyhole limpet hemocyanin conjugate of N-terminal Pra peptide DAPGDRMEEPLPDRAC-NH_2 (antibody N; HSV-37-93) and N-terminal ICP-35 peptide PTSGTPAPAPPGDGSC-NH_2 (antibody I; HSV-31-93) (Multiple Peptide Systems) as immunogens (Fig. 1).

Western blot analysis. Vero cells were infected at an MOI of 5 PFU/cell and harvested 14 h postinfection. The virus-infected Vero cell extracts were subjected to sodium dodecyl sulfate-polyacrylamide gel electrophoresis (12% cross-linker). Protein, 2.5 μg for the ICP-35 Western blots and 25 μg for the two Pra/N_0 Western blots, was loaded in each lane. Gels were transferred to Immobilon-P membranes (Millipore) and blocked in 1× phosphate-buffered saline–5% nonfat dry milk–0.1% Tween 20. Pra and ICP-35 were visualized with a two-antibody system. The first antibody was antibody I for the ICP-35 Western blots and antibody N for the Pra Western blots. The second antibody was goat anti-rabbit immunoglobulin G (heavy plus light chains) horseradish peroxidase conjugate (Sigma Chemical Company). Western blots were developed with an ECL kit from Amersham.

Sample preparation for TEM. Twenty hours postinfection Vero cells that were infected at an MOI of 5 PFU/cell were washed twice in phosphate-buffered saline, fixed with 1.0% glutaraldehyde in 1.0% cacodylate buffer (pH 7.5), scraped off of the flask, and pelleted. The cells were then washed in 1.0% cacodylate buffer for 1 h and postfixed for 1 h with 1.0% osmium tetroxide in 1.0% cacodylate buffer. The fixed samples were dehydrated with 50 to 100% ethanol in 10% steps of 15 min each and then transferred to 100% propylene

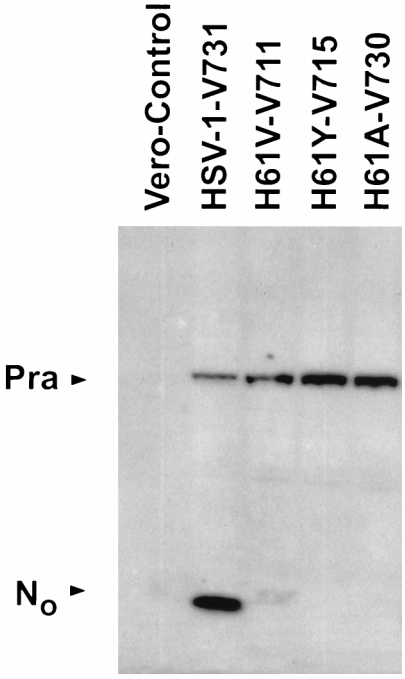

FIG. 2. N antibody, Western blot analysis of H61 mutant virus-infected Vero cell extracts. Vero cells were infected with virus at an MOI of 5 PFU/cell at 37°C and were harvested 14 h postinfection. Twenty-five micrograms of protein was loaded in each lane. Lane 1, mock-infected Vero cells; the other lanes are as indicated.

oxide for 15 min. The cells were pelleted, and the pellet was infiltrated with a 1:1 solution of propylene oxide and Epon (Poly Embed 12) overnight. The samples were then transferred to fresh Epon for 1 h and transferred into fresh Epon again. Cell pellets were polymerized at 37°C for 64 h and then transferred to a 56°C oven overnight. After polymerization, the embedded samples were sectioned at a thickness of 60 to 80 nm with a Riechert-Jung Ultracut E ultramicrotome. Sections were collected, mounted onto copper grids, and poststained with uranyl acetate and lead citrate. The grids were examined in a Hitachi HU-12A transmission electron microscope (TEM) at 85 kV (Advanced Biotechnologies Inc. in Columbia, Md.).

RESULTS

His61 mutations. Mutant HSV-1 viruses with point mutations at the conserved histidine residues of HSV-1 protease were constructed by using a previously described two-plasmid, four-cosmid system of mutagenesis (22) and characterized to assess the roles of these residues. All three of the H61 mutant viruses studied (H61V-V711, H61Y-V715, and H61A-V730) were unable to replicate in Vero cells at the tested temperatures, 31, 34, 37, and 39°C, but propagated on protease-expressing host range cell line PHS-23 (data not shown).

His61 Western blot analysis. The protease activities of the viruses with point mutations at H61 were assessed by Western blot analysis of infected Vero cell extracts, prepared 14 h postinfection. Western blots were developed with an antibody that recognizes the N-terminal domain of Pra (antibody N) or an antibody that recognizes the N terminus of ICP-35 (antibody I) (Fig. 1). Western blot analysis of virus-infected Vero cell extracts indicated that the H61 mutant viruses do not process either Pra to N_0 (Fig. 2) or ICP-35cd to ICP-35ef (Fig. 3).

His148 mutations: plaque morphology and temperature sensitivity. Viruses with mutations at H148 in Pra (H148A-V712, H148Y-V716, H148E-V728, and H148K-V729) exhibited a range of phenotypes. Two H148 mutants were viable in Vero cells. These mutants, H148A-V712 and H148E-V728, both exhibited a small-plaque phenotype when grown on Vero cells at 37 or 39°C. H148E-V728 grew more slowly than H148A-V712 and required 4 days of growth to reach a plaque size equivalent to that observed for H148A-V712 after 2 days of growth on Vero cells (at 37 or 39°C). When these two mutants were grown in host range cell line PHS-23, however, their plaque sizes and morphologies, 2 days postinfection, were found to be similar to those of parental strain HSV-1-V731 (data not shown). H148A-V712 showed no temperature sensitivity when grown at 31 to 39°C in Vero cells (Table 1), whereas H148E-V728 did not grow at 31 or 34°C.

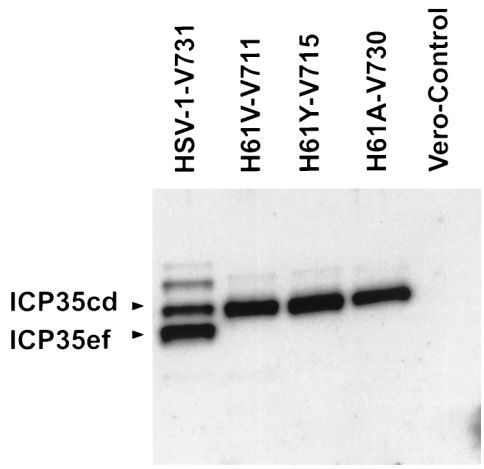

FIG. 3. I antibody, Western blot analysis of H61 mutant virus-infected Vero cell extracts. Vero cells were infected with virus at an MOI of 5 PFU/cell at 37°C and were harvested 14 h postinfection. Two and one-half micrograms of protein was loaded in each lane. Lane 5, mock-infected Vero cells; other lanes are as indicated.

One-step growth curves of H148A-V712 and H148E-V728. When these two mutants were grown on Vero cells at an MOI of 0.0005 PFU/cell (Fig. 4), the amount of virus produced per PFU at 20 h postinfection was found to be ~2 times lower for the H148A-V712 mutant and ~16 times lower for the H148E-V728 mutant virus than that observed for parental virus HSV-1-V731. At a high MOI (3 PFU/cell) H148A-V712 produced the same amount of virus as parental wild-type virus HSV-1-V731 at 20 h postinfection and H148E-V728 produced approximately three times less (Fig. 5).

Western blot analysis of H148A-V712 and H148E-V728. Vero cells were infected with mutant viruses at an MOI of 5 PFU/cell and were harvested 14 h postinfection. A Western

TABLE 1. HSV-1 protease histidine 148 mutant virus titers[a]

Mutant virus	Virus titers (PFU/ml) on:				
	Vero cells at:				PHS-23 cells at 37°C
	31°C	34°C	37°C	39°C	
H148A-V712	6.3×10^6	7.4×10^6	6.0×10^6	3.1×10^6	8.2×10^6
H148Y-V716	0	0	7.0×10^1	8.0×10^1	5.5×10^6
H148E-V728	0	0	9.8×10^6	7.5×10^6	6.8×10^6
H148K-V729	4.0×10^2	2.0×10^2	6.0×10^2	4.0×10^2	6.0×10^6
HSV-1-V731[b]	8.8×10^6	1.4×10^7	1.4×10^7	1.5×10^7	7.4×10^6

[a] Vero cells were infected at an MOI of 1 to 3 PFU/cell and then harvested, and titers were determined 18 h postinfection.

[b] HSV-1-V731 is an HSV-1 strain 17 virus with an F/17 Pra chimera that consists of the N_0 protease of HSV-1 strain F and the ICP-35 of HSV-1 strain 17. HSV-1-V731 is the parental strain of the H61 and H148 mutants.

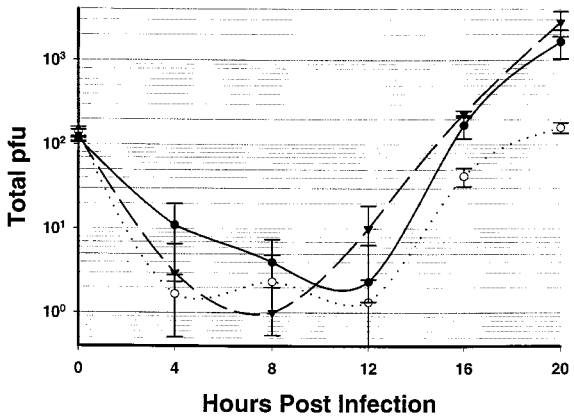

FIG. 4. Low-MOI one-step growth curves for H148A-V712 (●), H148E-V728 (○), and parental strain HSV-1-V731 (▼) at 37°C. Vero cells were infected at an MOI of 0.0005 PFU/cell, and the experiment was done in triplicate. The error bars indicate the standard deviation.

blot analysis of H148A-V712- or H148E-V728-infected cell extracts showed a reduced conversion of Pra to N_0 relative to that of the parental HSV-1-V731 strain as reflected in a comparison of the intensity of the Pra band relative to that of the N_0 band for each virus (Fig. 6). Processing of Pra to N_0 was at an approximately twofold-lower level for H148A-V712 than for H148E-V728; however, the processing of ICP-35cd to ICP-35ef by both H148A-V712 and H148E-V728 appeared similar, 14 h postinfection, to that of wild-type HSV-1-V731 (Fig. 7). Surprisingly, H148E-V728 is more attenuated than H148A-V712 and yet appears to process Pra to N_0 more efficiently than does H148A-V712. Further studies are required to determine the extent to which this result reflects the impact of the mutations at H148 on the nonproteolytic functions of the protease domain.

Western blot analysis of H148Y-V716 and H148K-V729. H148Y-V716 and H148K-V729 were not viable in Vero cells at any temperature tested (Table 1). Western blots of infected Vero cell extracts of mutant virus H148K-V729 (Fig. 6 and 7) indicated that H148K-V729, like the H61 virus mutants, did not process either Pra to N_0 or ICP-35cd to ICP-35ef. The Western blot of extracts of Vero cells infected with H148Y-V716 revealed greater than 25% protease activity in the conversion of Pra to N_0 (Fig. 6) 14 h postinfection, but the ICP-35 Western blots showed no processing of ICP-35cd to ICP-35ef (Fig. 7). The fact that mutant H148Y-V716 processed Pra to N_0 but failed to process ICP-35cd to ICP-35ef and was unable to replicate is consistent with the view that the processing of ICP-35cd to ICP-35ef is required for virus replication.

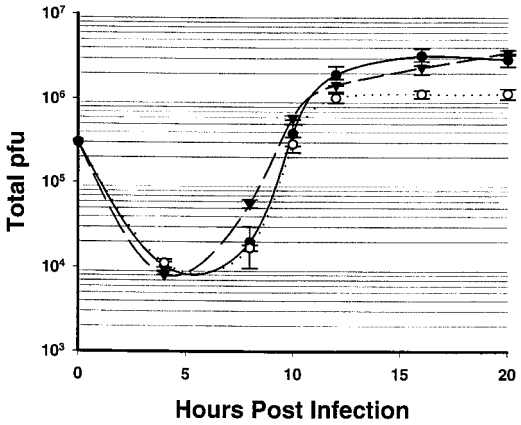

FIG. 5. High-MOI one-step growth curve of H148A-V712 (●), H148E-V728 (○), and parental strain HSV-1-V731 (▼) at 37°C. Vero cells were infected at an MOI of 3.0 PFU/cell, and the experiment was done in triplicate. The error bars indicate the standard deviation.

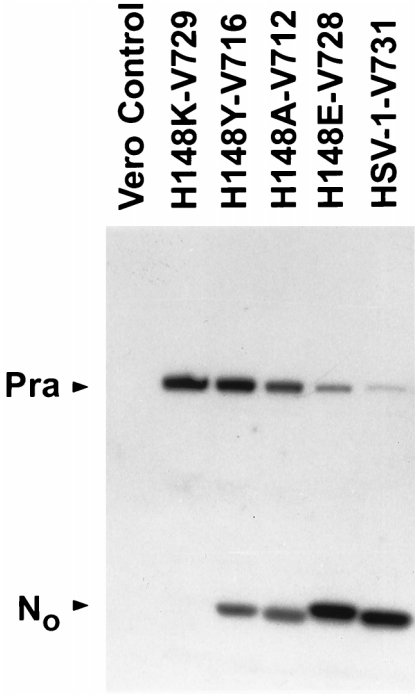

FIG. 6. N antibody, Western blot analysis of H148 mutant virus-infected Vero cell extracts. Vero cells were infected with virus at an MOI of 5 PFU/cell at 37°C and were harvested 14 h postinfection. Lane 1, mock-infected Vero cells; other lanes are as indicated.

Purity of H61 and H148 mutant viruses. Mutant viruses were plaque purified three times and then expanded on Vero

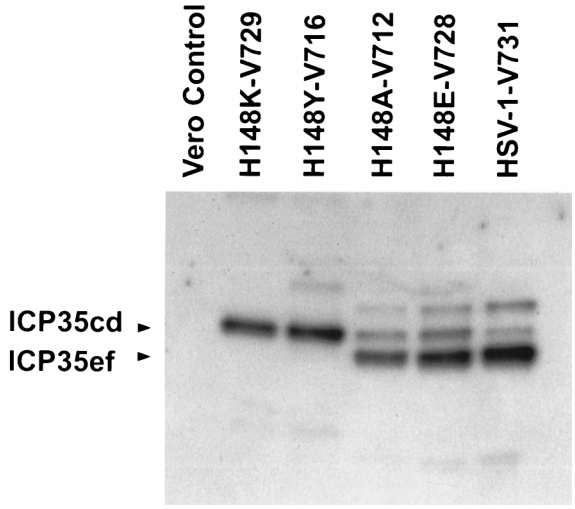

FIG. 7. I antibody, Western blot analysis of H148 mutant virus-infected Vero cell extracts. Vero cells were infected with virus at an MOI of 5 PFU/cell at 37°C and were harvested 14 h postinfection. Lane 1, mock-infected Vero cells; other lanes are as indicated.

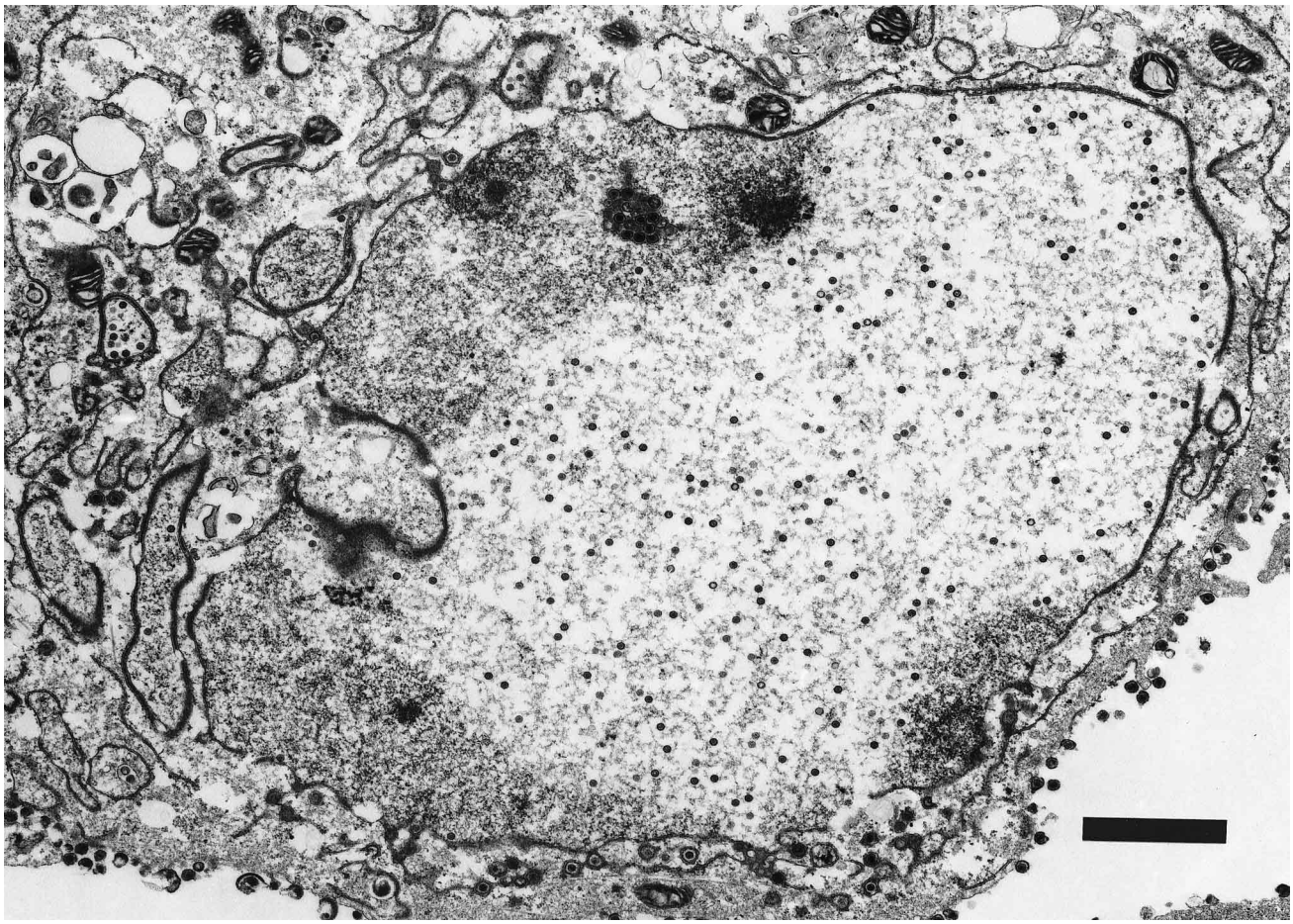

FIG. 8. TEM of Vero cell infected with HSV-1-V731 20 h postinfection. Magnification, ×9,600. Bar, 2 μm. The corresponding TEM of H148A-V712 was indistinguishable from that of HSV-1-V731 at 20 h postinfection (data not shown).

or PHS-23 cells. Southern blot analysis confirmed that the restriction site introduced with the His mutation was present in the isolated mutant viruses. Overexposure of the Southern blot did not reveal a wild-type HSV-1 contaminating virus band in the mutated DNA of H148A-V712 or H148E-V728 which grew on Vero cells (data not shown). Virus plaque sizes for these small-plaque phenotype His mutants were also measured on Vero cells, and the cells were observed to contain less than 0.01 percent virus with a large-plaque (wild-type virus) phenotype (data not shown).

The titers of the nonviable H61 and H148 mutants on both Vero and PHS-23 cells were measured to determine the amount of contaminating HSV-1 wild-type virus generated from homologous recombination with the PHS-23 Pra, spontaneous reversion, or possible second-site mutations. All of the viruses grown on PHS-23 cells contained a low titer of revertant virus that was less then 0.01 percent of the viral stock. When the titer rose above 0.01 percent the virus was plaque purified.

To determine whether the low titer of virus (obtained from nonviable virus stock solutions) that grew on Vero cells reflected leak through of the mutation or reversion to the wild-type phenotype, three plaques from each nonviable mutant grown on Vero cells were selected and expanded on PHS-23 cells and the titers on both Vero and PHS-23 cells were determined. All of the plaques grew to the same titer on Vero and PHS-23 cells (data not shown), suggesting that homologous recombination with the DNA in the host range cell line PHS-23 had occurred at a low frequency ($<10^{-4}$). The amount of wild-type virus increased with each passage of the virus mutant (data not shown). Gao et al. (8) reported a similar result with HSV-1 protease deletion mutant m100 when it was passaged on their host range cell line.

It is unlikely that the altered phenotypes associated with the H61 and H148 mutant viruses reflect the effects of a random second-site mutation, since repeated transfections (three or more for each mutant) yielded phenotypically identical viruses. Moreover, *Bsm*I fragments containing the protease-encoding domain, N_0, from H61A-V730 and H148A-V712 were subcloned from these mutant viruses, sequenced, and shown to encode only the expected Ala-for-His replacements with no second-site mutations.

TEM studies. (i) H61A-V730. TEM studies were undertaken to characterize a representative set of the mutant viruses with respect to capsid assembly and the intracellular localization of Pra and ICP-35cd and their processed products. Vero cells infected with parental virus HSV-1-V731 contained three types of capsids: empty A capsids, large-protein dense-core B capsids, and mature DNA-containing small-core C capsids as previously reported (Fig. 8) (19). In contrast, the proteolytically inactive strain, H61A-V730, contained only large symmetrical arrays of B capsids (Fig. 9) that appeared to emanate from the

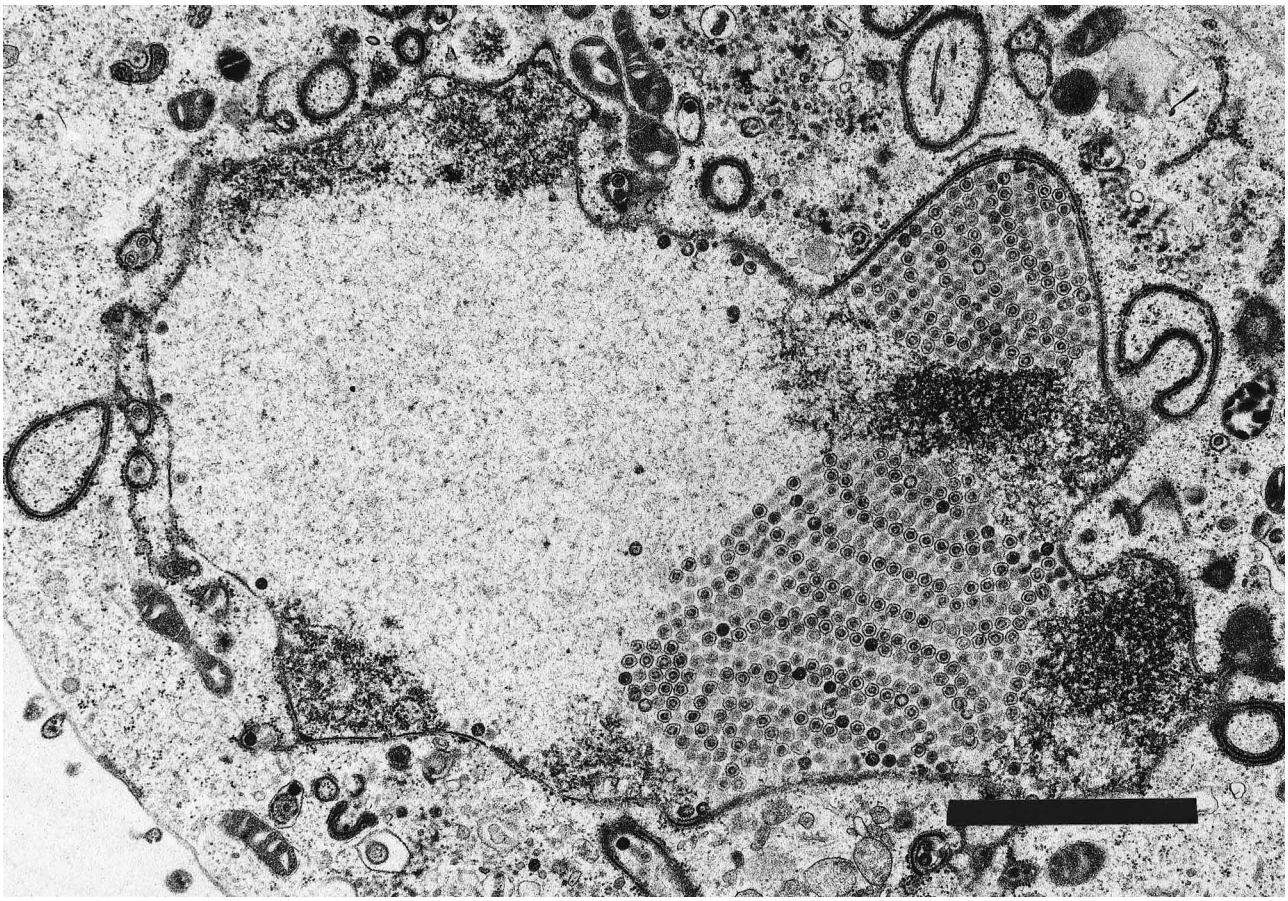

FIG. 9. TEM of Vero cells infected with H61A-V730 20 h postinfection. Shown are nuclear B capsids. Magnification, ×16,000. Bar, 2 μm.

nuclear membrane. However, no A or C capsids were observed in the nucleus. Extracellular spaces were filled with large numbers of L particles; however, no virus particles were observed in the extracellular spaces (data not shown).

(ii) H148E-V728. Examination by TEM of Vero cells infected with H148E-V728 at 20 h postinfection revealed a mixture of capsids at various stages of development. The nuclei of Vero cells infected with H148E-V728, 20 h postinfection, revealed that approximately 50% of the nuclear capsids were arranged in symmetrical arrays of B capsids emanating from the nuclear membrane (Fig. 10A). Interestingly, in the viral region of the nucleus where DNA packaging has been shown to occur (20), most of the capsids were covered with an electron-dense material that may be DNA (Fig. 10B). In addition, some of the B-capsid arrays had closely associated darkly stained complexes that may be DNA-packaging complexes (Fig. 10C). Interestingly, these complexes were not observed in either the H148A-V712 mutant or the HSV-1-V731 parental strain at 20 h postinfection. The remaining H148E-V728 nuclear capsids were monodispersed and similar in size to parental-strain HSV-1-V731 C capsids. (These and all other observed characteristics of the HSV-1-731 parental strain were indistinguishable from those of wild-type HSV-1 strain 17 virus.) Most of the capsids found in the cytoplasm did not have the condensed core characteristic of the HSV-1-V731 parental strain (data not shown). However, virus particles in the extracellular spaces were indistinguishable from those of the HSV-1-V731 parental strain (data not shown). The altered distribution relative to that of the HSV-1-V731 parental strain of intermediate capsids and virus assembly products seen with H148E-V728 at 20 h postinfection may reflect differences in the relative rates of individual steps in the capsid maturation pathway.

DISCUSSION

All three of the HSV-1 protease mutants with replacements at H61 (H61V-V711, H61Y-V715, and H61A-V730) were unable to replicate and did not process either Pra to N_0 or ICP-35cd to ICP-35ef. It might be argued that the processing of Pra to N_0 reflects *cis* cleavages that don't involve serine protease activity, whereas processing of ICP-35cd to ICP-35ef involves a serine protease-catalyzed *trans* cleavage. Regardless of whether only *trans* or both the *cis* and *trans* cleavages proceed via a serine protease mechanism, the observation that the H148A-V712 and H148E-V728 mutants are viable and exhibit both *cis* and *trans* cleavages excludes H148 as being essential for either proteolysis or virus viability.

The reports that the H148A-mutated HSV-1 protease lacked protease activity in both transient transfection and in *Escherichia coli* expression systems (5, 12, 28) appear to conflict with our observation of the processing of Pra to N_0 and of ICP-35cd to ICP-35ef in H148A-V712-infected Vero cells. It remains to be established whether the processing of Pra to N_0 and ICP-35cd to ICP-35ef that we observed in H148A-V712-infected Vero cells might reflect local concentration effects within the

A

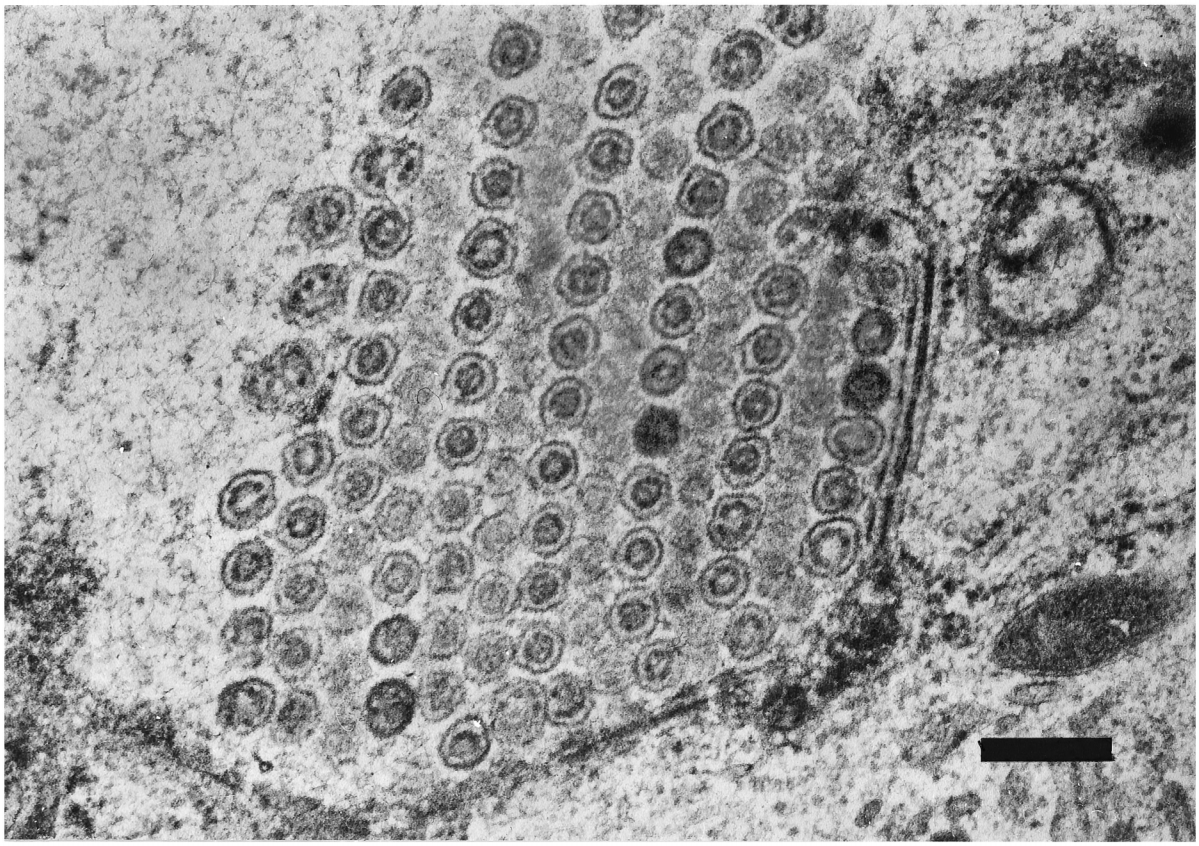

B

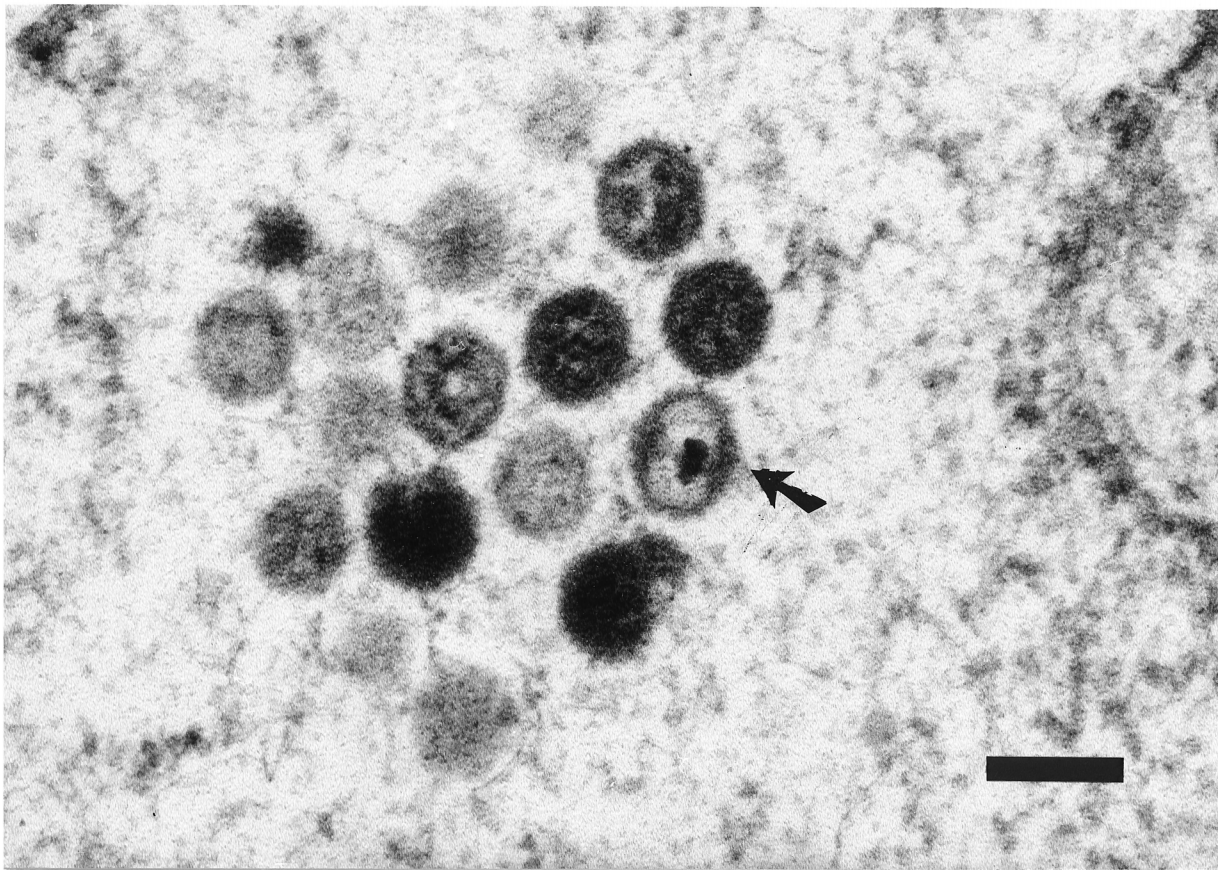

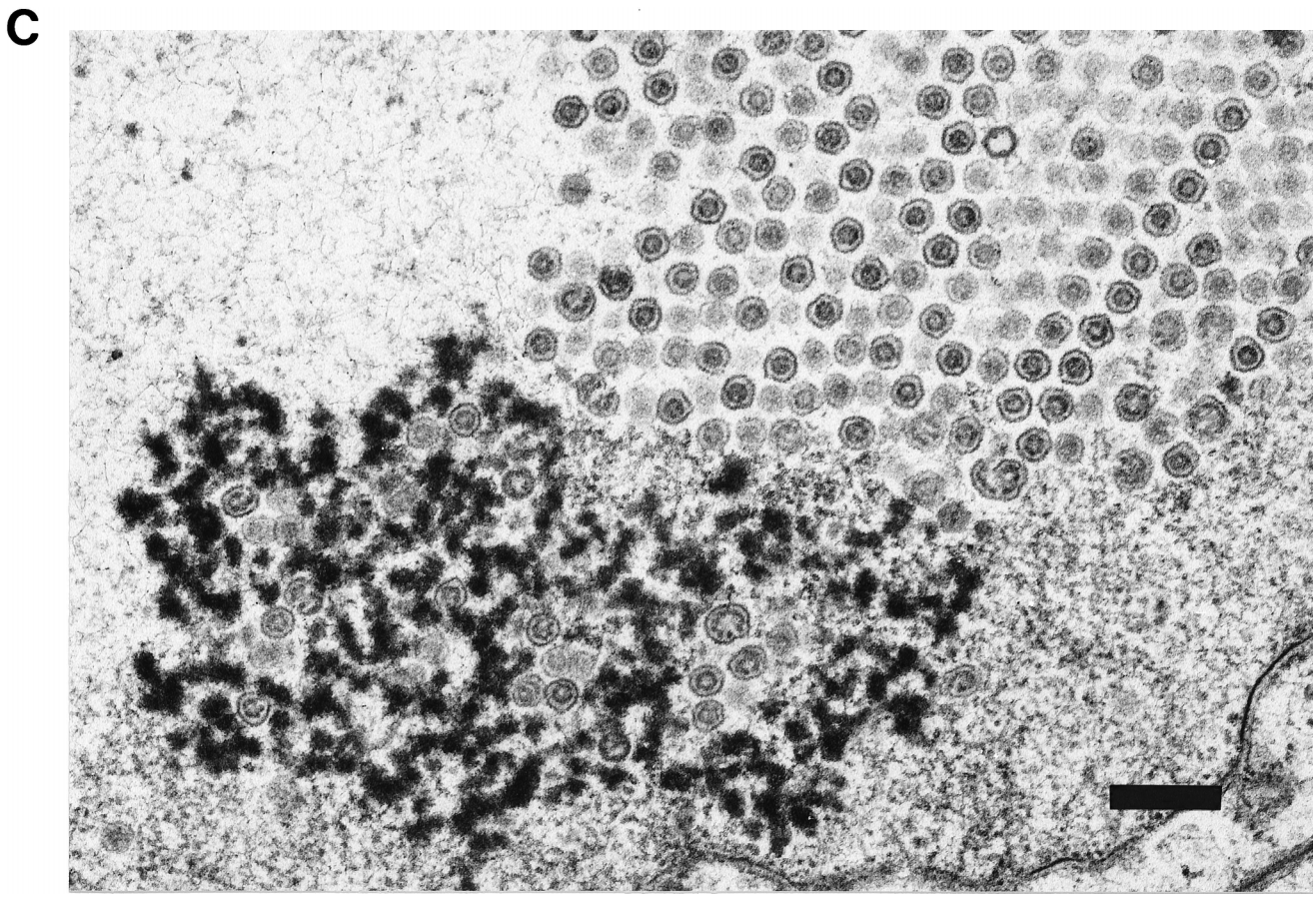

FIG. 10. TEM of Vero cells infected with H148E-V728. (A) Crystal-like arrays of B capsids lining the nuclear membrane. Magnification, ×64,800. Bar, 300 nm. (B) C capsid (arrow) adjacent to densely coated capsids. The densely stained material may be DNA. Magnification, ×96,000. Bar, 200 nm. (C) B capsids in crystal-like arrays dispersed in a densely stained area that may represent DNA packaging complexes. Magnification, ×38,400. Bar, 400 nm.

capsid or the presence of a viral cofactor of HSV-1 protease in the infected Vero cells.

TEM studies of a representative H61 nonviable mutant, H61A-V730, showed an accumulation of highly symmetrical arrays of B capsids in the nuclei of infected Vero cells. H148E-V728-infected Vero cells also accumulated symmetrical arrays of B capsids; however, these capsid arrays were smaller than those seen with H61A-V730. Interestingly, near the edges of the H148E-V728 capsid arrays, the B capsids were less well packed. This dissociation is most pronounced near areas of densely stained material that may represent DNA packaging complexes (Fig. 10C). These densely stained complexes did not accumulate in Vero cells infected with parental strain HSV-1-V731. It is our contention that the capsid arrays observed in the electron micrographs (Fig. 10A and C) of H148E-V728-infected Vero cells are also intermediates in the maturation of wild-type virus capsids and that the abnormal build-up of these intermediates observed with H148E-V728 is due in part to the attenuated protease activity of this mutant virus. In this regard it is interesting to note that a TEM of wild-type HSV-1 published by Roizman and Spear (23) depicts the presence of symmetrical arrays of wild-type HSV-1 virus early in infection.

Our ability to produce an attenuated virus by a point mutation that incrementally reduces the activity of HSV-1 protease is consistent with the possibility that protease processing may be a rate-controlling step in the pathway for virus maturation. The observation that H148E-V728 was more attenuated than H148A-V712 in spite of the fact that H148-V728 appeared to process Pra to N_0 more efficiently than did H148A-V712, however, suggests the possibility that the H148E mutation may impact virus growth rate via its effects on the structural role of Pra as a constituent of the protein scaffold for assembly of virus capsids. Alternatively, the rate of DNA packaging may be inhibited by the mutation as evidenced by the buildup of what appears to be DNA-packaging complexes (Fig. 10B and C). These putative DNA-packaging complexes were not observed in TEM studies of the mutant H148A-V712 strain or of the HSV-1-V731 parental strain. At 20 h postinfection these virus strains had matured past the DNA-packaging stage to mature monodispersed virus particles in the nucleus as illustrated in Fig. 5 depicting HSV-1-V731. Further studies are required, however, to determine the altered interactions responsible for the attenuated growth induced by H148E-V728. H148Y-V716 was active against Pra, though nonviable, when grown on Vero cells. This lack of viability may reflect the inability of H148Y-V716 to process ICP-35cd and/or may be an effect of the mutation on the interactions of Pra in the protein scaffold. Not surprisingly, H148K-V729 cleaved neither Pra nor ICP-35cd and was also not viable.

The observation that all of the H61 mutations resulted in a loss of both *cis* and *trans* cleavage activity supports the contention that H61 is essential for proteolytic activity and that this residue is probably the catalytically essential His, provided, of course, that HSV-1 protease, like hCMV protease and other serine proteases, utilizes an active-site histidine residue as a general acid or base catalyst of proton transfer from the hy-

droxyl group of the active-site serine residue to the leaving group of the substrate. It remains, however, for X-ray crystallographic analysis of HSV-1 protease to establish the spatial proximity of H61 to the active-site serine (S129) required by the putative role of H61 in catalysis.

The recent unanticipated observation (2, 21, 24, 27) indicating that hCMV protease is devoid of a catalytic aspartic or glutamic acid residue reveals the potential for alteration of the signature catalytic triad of serine proteases. It has been suggested (2, 21, 24, 27), based on the structure of hCMV protease, that H157 may be functionally equivalent to the active-site aspartic acid residue in orienting the active-site histidine residue so that it can efficiently transfer a proton from the active-site serine residue to the leaving group of the substrate. The active-site histidine residue (H63) of hCMV protease, however, may not enjoy an optimal alignment for catalysis. Whereas the replacement of the active-site aspartic acid residue with an alanine residue in the serine protease subtilisin results in a 5×10^4-fold reduction in the specificity constant (k_{cat}/K_m) (1), replacement of H157 with an alanine residue in hCMV protease results in only a 15- to 30-fold reduction in catalytic activity (27). Consistent with our contention that the H63 of hCMV protease may not be optimally aligned for catalysis is the observation that the value of the specificity constant for hydrolysis of a peptide analog of the natural substrate of hCMV is only 4,000 M^{-1} s^{-1} (4), whereas highly specific proteases such as thrombin (9) exhibit specificity constants of $\sim 10^7$ M^{-1} s^{-1} that reflect the fact that they have evolved to a state wherein the rate of diffusional collision of enzyme and substrate rather than the rate of chemical catalysis limits the rate of the enzymically catalyzed reaction. The observation (27) that substitution of an aspartic or glutamic acid residue for H157 in hCMV protease results in a 5- to 10-fold reduction in activity suggests that it may not be possible to effect optimal alignment of H63 for catalysis by the simple substitution of an acidic amino acid residue for H157 in hCMV protease.

One might ask why hCMV protease and perhaps other herpes proteases have not evolved (as have other highly specific serine proteases) to a state of "catalytic perfection" wherein the rate of chemical catalysis is no longer rate limiting. In this regard, it should be noted that the cellular concentration of the protease Pra might be dictated by the structural role of Pra in the maintenance of the scaffold for assembly of the virus capsid. This structural constraint, which fixes the amount of Pra required for virus assembly, may well remove evolutionary pressure to increase catalytic efficiency so as to reduce the requirement for enzyme biosynthesis. In fact, an increase in catalytic efficiency beyond a certain point might be deleterious, since it might result in premature cleavage of Pra. Thus, the second conserved histidine of herpes proteases may serve as a modulator of catalytic activity to ensure that the activity of the enzyme is optimized for timely cleavage of Pra in the context of the virus rather than for maximal catalytic activity.

The properties of the H148 mutant viruses characterized in the present study are consistent with the conserved H148 residue of HSV-1 protease being an important determinant of virus maturation via its effects on catalytic efficiency and substrate specificity. Further studies are required to establish the relative importance of the regulation of catalytic efficiency and/or substrate specificity of HSV-1 protease by H148 via its interaction with H61, its interactions with Pra substrates, its effect on the conformation of Pra, and its effect on the monomer-to-dimer conversion that has been recently associated with protease activation (4, 15).

ACKNOWLEDGMENTS

We thank Gary Cohen from the University of Pennsylvania School Of Dental Medicine for helpful suggestions and insightful discussions. We also are happy to acknowledge the technical assistance of Bohdan Wolanski of Merck Research Laboratories and John Bernbaum of Advanced Biotechnologies Inc. in the preparation and examination of samples for the electron microscopy studies.

REFERENCES

1. **Carter, P., and J. A. Wells.** 1988. Dissecting the catalytic triad of a serine protease. Nature **332:**564–568.
2. **Chen, P., H. Tsuge, R. J. Almassy, C. L. Gribskov, S. Katch, D. L. Vanderpool, S. A. Margosiak, C. Pinko, D. A. Matthews, and C.-C. Kan.** 1996. Structure of the human cytomegalovirus protease catalytic domain reveals a novel serine protease fold and catalytic triad. Cell **86:**835–843.
3. **Cunningham, C., and A. J. Davison.** 1993. A cosmid-based system for constructing mutants of herpes simplex virus type 1. Virology **197:**116–124.
4. **Darke, P. L., J. L. Cole, L. Waxman, D. L. Hall, M. K. Sardana, and L. C. Kuo.** 1996. Active human cytomegalovirus protease is a dimer. J. Biol. Chem. **271:**7445–7449.
5. **Deckman, I. C., M. Hagen, and P. J. McCann III.** 1992. Herpes simplex virus type 1 protease expressed in *Escherichia coli* exhibits autoprocessing and specific cleavage of the ICP35 assembly protein. J. Virol. **66:**7362–7367.
6. **Desai, P., S. C. Watkins, and S. Person.** 1994. The size and symmetry of B capsids of herpes simplex virus type 1 are determined by the gene products of the UL26 open reading frame. J. Virol. **68:**5365–5374.
7. **Dilanni, C. L., J. T. Stevens, M. Bolgar, D. R. O'Boyle II, S. P. Weinheimer, and R. J. Colonno.** 1994. Identification of the serine residue at the active site of the herpes simplex virus type 1 protease. J. Biol. Chem. **269:**12672–12676.
8. **Gao, M., L. Matusick-Kumar, W. Hurlburt, S. F. DiTusa, W. W. Newcomb, J. C. Brown, P. J. McCann III, I. Deckman, and R. J. Colonno.** 1994. The protease of herpes simplex virus type 1 is essential for functional capsid formation and viral growth. J. Virol. **68:**3702–3712.
9. **Higgins, D. L., S. D. Lewis, and J. A. Shafer.** 1983. Steady state kinetic parameters for the thrombin-catalyzed conversion of human fibrinogen to fibrin. J. Biol. Chem. **258:**9276–9282.
10. **Higuchi, R.** 1990. Recombinant PCR, p. 177–183. *In* M. A. Innis, D. H. Gelfand, J. J. Sninsky, and T. J. White (ed.), PCR protocols. Academic Press, Inc. San Diego, Calif.
11. **Laemmli, U. K.** 1970. Cleavage of structural proteins during the assembly of the head of bacteriophage T4. Nature **227:**680–685.
12. **Liu, F., and B. Roizman.** 1992. Differentiation of multiple domains in the herpes simplex virus 1 protease encoded by the U_L26 gene. Proc. Natl. Acad. Sci. USA **89:**2076–2080.
13. **Liu, F., and B. Roizman.** 1991. The promoter, transcriptional unit, and coding sequence of herpes simplex virus 1 family 35 proteins are contained within and in frame with the U_L26 open reading frame. J. Virol. **65:**206–212.
14. **Liu, F., and B. Roizman.** 1991. The herpes simplex virus 1 gene encoding a protease also contains within its coding domain the gene encoding the more abundant substrate. J. Virol. **65:**5149–5156.
15. **Margosiak, S. A., D. L. Vanderpool, W. Sisson, C. Pinko, and C.-C. Kan.** 1996. Dimerization of the human cytomegalovirus protease: kinetic and biochemical characterization of the catalytic homodimer. Biochemistry **35:** 5300–5307.
16. **Matusick-Kumar, L., W. Hurlburt, S. P. Weinheimer, W. W. Newcomb, J. C. Brown, and M. Gao.** 1994. Phenotype of the herpes simplex virus type 1 protease substrate ICP35 mutant virus. J. Virol. **68:**5384–5394.
17. **Newcomb, W. W., and J. C. Brown.** 1991. Structure of the herpes simplex virus capsid: effects of extraction with guanidine hydrochloride and partial reconstitution of extracted capsids. J. Virol. **65:**613–620.
18. **Newcomb, W. W., B. L. Trus, F. P. Booy, A. C. Steven, J. S. Wall, and J. C. Brown.** 1993. Structure of the herpes simplex virus capsid. Molecular composition of the pentons and the triplexes. J. Mol. Biol. **232:**499–511.
19. **Nii, S.** 1992. Electron microscopic study on the development of herpesviruses. J. Electron Microsc. **41:**414–423.
20. **Puvion-Dutilleul, F., and E. Puvion.** 1989. Ultrastructural localization of viral DNA in thin sections of herpes simplex virus type 1 infected cells by in situ hybridization. Eur. J. Cell Biol. **49:**99–109.
21. **Qiu, X., J. S. Culp, A. G. DiLella, B. Hellmig, S. S. Hoog, C. A. Janson, W. W. Smith, and S. S. Abdel-Meguid.** 1996. Unique fold and active site in cytomegalovirus protease. Nature **383:**275–279.
22. **Register, R. B., and J. A. Shafer.** 1996. A facile system for construction of HSV-1 variants: site directed mutation of the UL26 protease gene in HSV-1. J. Virol. Methods **57:**181–193.
23. **Roizman, B., and P. G. Spear.** 1973. Herpesviruses, p. 83–107. *In* A. J. Dalton and F. Haguenau (ed.), Ultrastructure of animal viruses and bacteriophages, an atlas. Academic Press, New York, N.Y.
24. **Shieh, H.-S., R. G. Kurumbail, A. M. Stevens, R. A. Stegeman, E. J. Sturman, J. Y. Pak, A. J. Wittwer, M. O. Palmier, R. C. Wiegand, B. C. Holwerda, and W. C. Stallings.** 1996. Three-dimensional structure of human cytomegalovirus protease. Nature **383:**279–282.

25. **Tatman, J. D., V. G. Preston, P. Nicholson, R. M. Elliott, and F. J. Rixon.** 1994. Assembly of herpes simplex virus type 1 capsids using a panel of recombinant baculoviruses. J. Gen. Virol. **75:**1101–1113.
26. **Thomsen, D. R., L. L. Roof, and F. L. Homa.** 1994. Assembly of herpes simplex virus (HSV) intermediate capsids in insect cells infected with recombinant baculoviruses expressing HSV capsid proteins. J. Virol. **68:**2442–2457.
27. **Tong, L., C. Qian, M.-J. Massariol, P. R. Bonneau, M. G. Cordingley, and L. Lagace.** 1996. A new serine-protease fold revealed by the crystal structure of human cytomegalovirus protease. Nature **383:**272–275.
28. **Weinheimer, S. P., P. J. McCann III, D. R. O'Boyle II, J. T. Stevens, B. A. Boyd, D. A. Drier, G. A. Yamanaka, C. L. Dilanni, I. C. Deckman, and M. G. Cordingley.** 1993. Autoproteolysis of herpes simplex virus type 1 protease releases an active catalytic domain found in intermediate capsid particles. J. Virol. **67:**5813–5822.
29. **Welch, A. R., L. M. McNally, M. R. T. Hall, and W. Gibson.** 1993. Herpesvirus proteinase: site-directed mutagenesis used to study maturational, release, and inactivation cleavage sites of precursor and to identify a possible catalytic site serine and histidine. J. Virol. **67:**7360–7372.